



# Copper and silver selenide crystal growth rate measurements as a method for determination of ionic conductivity

Zlatko Vučić<sup>a</sup>, Davorin Lovrić<sup>a</sup>, Jadranko Gladić<sup>a,\*</sup>, Božidar Etlinger<sup>b</sup>

<sup>a</sup> *Institute of Physics, Bijenička cesta 46, P.O. Box 304, Zagreb HR 10000, Croatia*

<sup>b</sup> *Ruđer Bošković Institute, Bijenička cesta 54, P.O. Box 180, Zagreb 10000, Croatia*

Received 25 July 2003; accepted 7 November 2003

Communicated by G.B. Stringfellow

## Abstract

The motivation behind this work is the discrepancy between the measured and calculated growth rates of copper selenide spherical single crystals between 740 and 800 K. The growth of cylindrical polycrystalline samples of copper selenide at high temperatures was monitored in experiments that enabled full control of the geometry of growth. Together with the calculations based on Yokota's transport equation, these measurements eliminated ionic conductivity data as a possible reason behind too high values of the calculated growth rates. The equivalent growth experiments on polycrystalline silver selenide samples were performed as a test of the method, yielding excellent agreement with the results obtained by extrapolation of existing data. On the basis of these measurements and associated analysis, this method is proposed as a method for determination of ionic conductivity of mixed superionic conductors on temperatures up to the temperatures of melting, i.e. in the range in which other methods of ionic conductivity measurements either do not work or are not accurate enough.

© 2003 Elsevier B.V. All rights reserved.

PACS: 66.10.Ed; 66.30.Dn; 81.10.-h

Keywords: A1. Equilibrium crystal shape; A1. Growth rate; A1. Ionic conductivity; A2. Crystal growth; B2. Superionic conductors

## 1. Introduction

Recently discovered new growth modes of the facets of <sup>4</sup>He single crystals of nearly equilibrium shape (ECS) make the magnitude of the volume growth rate or its average 1D equivalent excep-

tionally important [1]. We searched for these growth modes at silver and copper chalcogenides belonging to a group of superionic conductors having high metal atoms diffusivity. These materials, together with <sup>4</sup>He crystals, belong to the small group of crystals that exhibit ECS [2,3] up to the centimeter sizes.

We have recently investigated the growth of cuprous selenide Cu<sub>2-δ</sub>Se single crystals between 740 and 800 K using improved Ohachi's growth method [4]. In these experiments at given and fixed temperature, the constant chemical potential

\*Corresponding author. Tel.: +38514698809; fax: +38514698889.

E-mail addresses: [vucic@ifs.hr](mailto:vucic@ifs.hr) (Z. Vučić), [lovric@ifs.hr](mailto:lovric@ifs.hr) (D. Lovrić), [gladic@ifs.hr](mailto:gladic@ifs.hr) (J. Gladić), [etlinger@rudjer.irb.hr](mailto:etlinger@rudjer.irb.hr) (B. Etlinger).

difference is established along the growing crystal by fixing chemical potentials at its both ends: by the copper metal disc, which serves as a source of copper atoms that diffuse along the sample toward its growing interface at the non-growing end, and by the selenium vapor pressure, which is in turn the equilibrium pressure of the certain preselected sample composition at the growing end. The experimental setup and the growing conditions were discussed in Ref. [4].

The growth process is described by Yokota's atom transport equation [5] under stationary conditions of time independent or slowly changing composition and/or chemical potential gradient distribution along the bulk sample from the metal copper contact end of the polycrystalline sample ( $\mu_{\text{Cu}_2\text{Se}} = \mu_0$ ), through the capillary orifice (single crystal seed selector) to the growing spherical single crystal surface ( $\mu_{\text{Cu}_{1.75}\text{Se}} = \mu_G$ )

$$\mu_0 - \mu_G = e^2 \frac{dn}{dt} \int_0^G \frac{dx}{\sigma_i(x)S(x)}, \quad (1)$$

where  $G$  denotes the growing interface. Due to the cylindrical symmetry, the ionic conductivity  $\sigma_i$ , and the cross-sectional area  $S$  depend on the axial coordinate  $x$ .  $S(x) = \pi r_{\text{in}}^2(x)$  is determined by the inner diameters of quartz tube within which the crystal grows except for the part of the growing crystal that grows on the top of the capillary tip in free space having spherical shape. The dependence of ionic conductivity  $\sigma_i$  on  $x$  is not known, since  $\sigma_i$  depends on the composition [6,7], the distribution of which along the grown sample is not known as well.

As discussed in Ref. [4], Cu atom current ( $dn/dt$ ) is up to 0.2% independent on the size of the spherical single crystal since the main drop of chemical potential difference occurs around the capillary orifice. To solve integral (1), we did serious approximations in Ref. [4] related to  $S(x)$  and to  $\sigma_i$  vs.  $x$  dependence reflecting the expected chemical potential i.e., Cu atom concentration dependence throughout the sample [6]. The solution obtained has shown that the copper atom current, or the volume growth rate,  $dV/dt$ , is given by

$$\frac{dV}{dt} = \frac{EMF \sigma_{iG} \Omega_{\text{Cu}}}{e GF}, \quad (2)$$

where  $EMF = (\mu_0 - \mu_G)/e$ ,  $\sigma_{iG}$  and  $\Omega_{\text{Cu}} = a^3/(4 \times 1.75)$  depend on growth temperature  $T_G$  and growth concentration  $\delta_G$ , while  $GF$  is geometrical factor specific of the particular experimental geometry.

The comparison between measured growth rates and the calculated ones, using the extrapolated values of  $EMF$ ,  $\sigma_{iG}$ ,  $\Omega_{\text{Cu}}$ , and by using as good as possible  $GF$ , revealed the disagreement [4]. The calculated values appear to be overestimated by a factor of 2.2 (cf. Fig. 10 in Ref. [4]). This result is the main motivation for the present investigation.

One or more of the following may cause this overestimate. One, the sample cross-section is smaller than the capillary interior [4]. Two, surface regions that are atomically flat (111) facets can have their growth rate limited by layer nucleation. Three, inaccurate ionic conductivities were used. Apparently, there are no reliable data on  $\sigma_i$  above 513 K while our growth experiments are performed at around  $(770 \pm 50)$  K. We therefore extrapolated the data for temperatures up to 513 K [6] to our growth temperatures.

To resolve the problem, or at least to reduce the number of possible causes for disagreement, we performed the growth experiments with well-defined geometry to minimize errors in determination of  $S(x)$ . Also, by growing samples in polycrystalline form we expect to eliminate or at least diminish the possible effect of nucleation resistance. Therefore, if we would indeed succeed to eliminate all causes but one by suitably adjusting the experimental setup, the method might be used as an alternative experimental method for ionic conductivity measurement.

The plan of the paper is as follows. We first describe the experimental setup that we used in our method of crystal growth and the procedure of acquisition and processing of data. After that we derive the equation describing the growth of our crystals. We then fit our data to the derived equations, first the data on copper selenide, and then the silver selenide data, which we used as a control system. From the results of the fitting procedure we deduce and discuss the magnitude of the ionic conductivity. The very end of the paper is devoted to our conclusions and to the brief discussion.

## 2. Experimental conditions

The growth experiments do not differ much from the ones described in Ref. [4], i.e., they were performed in an evacuated and sealed quartz ampoule situated in vertical transparent two-zone furnace (see Fig. 1 in Ref. [4]). The only difference is the geometry of the quartz tube inside the growth ampoule (instead of the quartz tube with capillary ending used in Ref. [4]). The real shape of the ampoule and the schematics of its inner tube are shown in Fig. 1.

Two versions of the inner tube are presented in Fig. 1, and both were used in experiments. The inner diameters of the quartz tubes along which the crystals grew were either 1 or 2 mm. All objects (metal Cu disc/cylinder and polycrystalline  $\text{Cu}_{2-\delta}\text{Se}$  sample) placed above  $x = 0$  were put into inner tube before the growth started. The sample grows starting at  $t = 0$  and  $x = 0$ , and at some time instant  $t$  it reaches the length  $x = L$ . We note that the sample initially (between  $x = 0$  and  $x_1$ ) grows by sprouting thin crystal threads [4,8,9]. The cross-section is therefore effectively very low when the growth starts and gradually reaches the full inner quartz tube cross-sectional area at  $x = x_1$ . According to our experience, this part of

the sample comprises at most 1 mm of the fully grown sample.

Prior to growth, the temperature distribution within the furnace was measured by inserting the Pt-Pt13%Rh thermocouples in a hollow growth ampoule. Our setup enabled at all times more than 15 mm long region of temperature axial homogeneity and constancy (within  $\pm 0.25$  K). The procedure of activating the growth process by raising the temperature of the Se reservoir and the crystal growth area is described in Ref. [4]. The temperatures within the furnace were monitored continuously during the experiments and after achieving the preset values (within about an hour) for crystal growth were kept constant within  $\pm 2$  K.

A typical growth experiment lasted for about 15 h, during which the growing crystal filled up about 15 mm length of the inner quartz tube (a few mm of the sprouting part and around 10 mm of the homogeneous crystal completely filling the interior of the quartz tube).

The growth was monitored by taking pictures of the growing crystal at the rate of 6–12 frames per minute by the CCD camera (Pulnix TM-765, with resolution of 756(H)  $\times$  581(V) and 256 levels of gray) mounted as an ocular to a Technival 2000

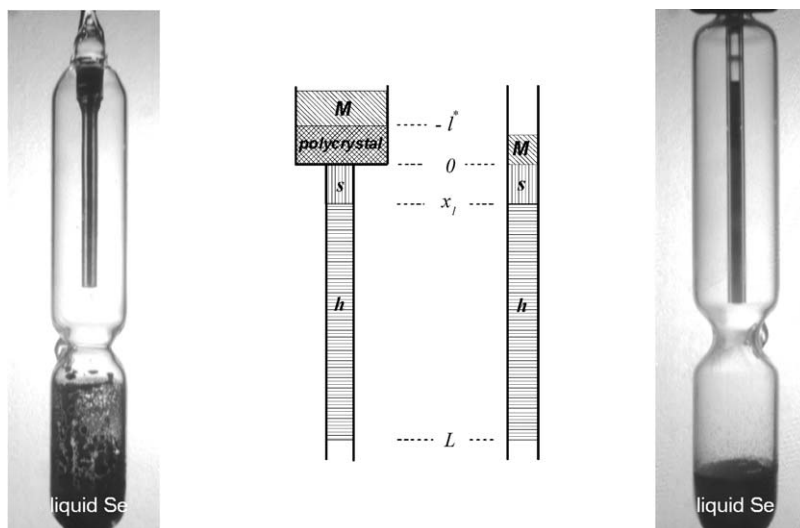


Fig. 1. Photographs and schematics of the quartz ampoules used in silver selenide (left) and copper selenide (right) growth experiments. *M*, *s* and *h* stand for metal, sprouting and homogeneous part, respectively.

microscope (which enabled us a magnification factor of 16). The signals from the camera were digitized and fed to computer by Matrox PIP-512B frame grabber making a sequence of frames representing the advantage of crystal face. A typical picture showing the silhouette of the growing crystal within the ampoule illuminated by a diffuse light from behind is shown in Fig. 2. The position of the crystal-gas boundary at each time instant was determined by subtracting the intensities of the previous frame from the current one for each pixel on the  $512 \times 512$  pixels grid. By doing this one obtains a frame with a distinct narrow dark strip, having a width of at most 1–2 pixels, on an otherwise light background. The precise position of the boundary within the narrow dark strip for each pixel in the direction perpendicular to the axis of growth was then obtained by determining the two maxima of the derivative of the gray level, corresponding to the two edges of a narrow dark strip, for this particular pixel, and by putting the real boundary in the middle between these two maxima, giving us a subpixel accuracy in determination of the boundary position. By subtracting the so obtained boundaries of two successive frames we determined the relative displacement of the crystal-gas boundary for each pixel on the axis perpendicular to the axis of growth. We note that these displacements consti-

tute a straight line, perpendicular to the direction of growth, even if the original crystal-gas surface is not perfectly flat, which makes the determination of the average displacement (i.e., of the velocity) of the crystal face much easier and more precise.

### 3. Equation of growth

In spite of the altered geometry of growth, Yokota's Eq. (1) is still useful. By splitting the geometrical factor in three parts (see Fig. 1) we obtain

$$\mu_0 - \mu_G = e^2 \frac{dn}{dt} \left( \int_{-l^*}^0 \frac{dx}{S_3 \sigma_i(x)} + \int_0^{x_1} \frac{dx}{S_1(x) \sigma_i(x)} + \int_{x_1}^L \frac{dx}{S_2 \sigma_i(x)} \right). \quad (3)$$

The first term in the sum is relevant only if the growth is initiated by the help of polycrystalline cylinder (of cross-section  $S_3$  and height  $l^*$ ). Irrespective of the source of Cu atoms (the bare Cu disc or Cu with polycrystalline Cu–Se sample), the initial sprouting of thin crystal threads inevitably occurs [4]. The nucleation resistance has been neglected throughout this work, since the sprouting provides a very high level of polycrystallinity.

By assuming that each Cu atom emerging from the interface creates at the growing surface the excess volume  $\Omega_{\text{Cu}} = a^3/7$ , one obtains  $\Omega_{\text{Cu}} dn = dV = S_2 dL$ , where  $a$  is the lattice parameter, and for  $\delta_G = 0.25$  there are 7 Cu atoms per unit cell.

To further simplify the calculations several approximations are made. First, we assume that the cross-section  $S_1(x)$  in the sprouting part of the grown sample, from 0 to  $x_1$ , can be approximated by its effective average value  $\bar{S}_1$ , which will be treated as a fitting parameter. Second, we use very accurate empirical functional dependence  $\sigma_i(x)^{-1}$  vs.  $\delta(x)$ , based on the ionic conductivity data [6] (cf. Fig. 3 in that paper), i.e.,

$$\frac{\sigma_i(\delta(x))}{\sigma_{\text{im}}(\delta_G)} = 2 \left( 1 + \left( \frac{\delta(x)}{\delta_G} \right)^\alpha \right)^{-1}, \quad (4)$$

where  $\delta(x)$  denotes the dependence of the deviation from stoichiometric content of Cu atoms per

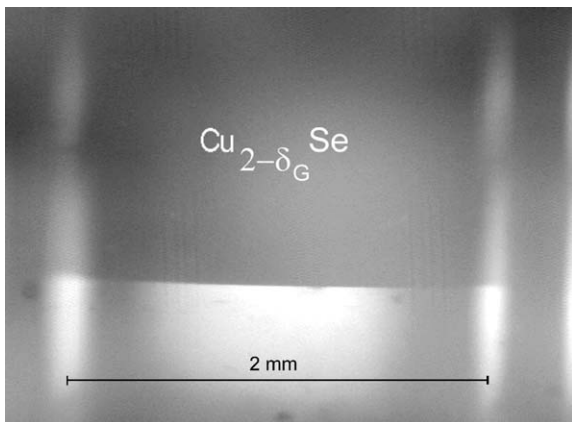


Fig. 2. A typical picture of the growing crystal (copper selenide). The ampoule has been illuminated by diffuse light from the backside.

molecule on the axial coordinate and  $\delta_G$  is its preselected (by Se vapor pressure) value at growing interface (0.25 in this case). The reasons for using this relation are as follows: (a) It is much easier to visualize the approximate composition dependence  $\delta(x)$  vs.  $x$  along the grown sample than the dependence of  $\sigma_i(x)$  vs.  $x$ . Namely,  $\delta(x)$  monotonically scales both from the non-growing end of sample ( $\delta(0) = 0$ ) to the end of the sprouting part ( $\delta(x) = 1$ ), reflecting the realistic behavior of  $S_1(x)$ , and throughout the rest of the grown sample, from  $x_1$  to  $x = L$  ( $\delta(L) = \delta_G$ ). (b) Using the empirical relation (4) the integration becomes much simpler. Using the known proportionality  $\mu(\delta(x)) \propto \delta(x)^{2/3}$ , the solution of integral (3) becomes straightforward. The exponent  $\alpha$  is found to be 0.775 and 0.825 for 452 K and 520 K, respectively, cf. Fig. 3. It may then take any value

in the interval defined by these values provided it is intrinsically temperature independent.

To solve integrals in Eq. (3) we assume a linear  $\delta(x)$  vs.  $x$  dependence in both parts of the grown sample, the sprouting one (I), and the homogenous one (II), i.e.,

$$\delta(x)_I = \delta(x_1) \left( \frac{x_1}{x} \right),$$

$$\delta(x)_{II} = \delta(x_1) + (\delta_G - \delta(x_1)) \frac{x - x_1}{L - x_1}. \quad (5)$$

We note that  $\delta(x_1)$  depends on length of the grown crystal  $L$ , changing from  $\delta(x_1) = \delta_G$  for  $L = x_1$ , to  $\delta(x_1) \approx 0$  for very large  $L$ . In the case of growth of Cu–Se system we have omitted the polycrystalline sample located between  $-l^*$  and 0 and then only last two integrals persist

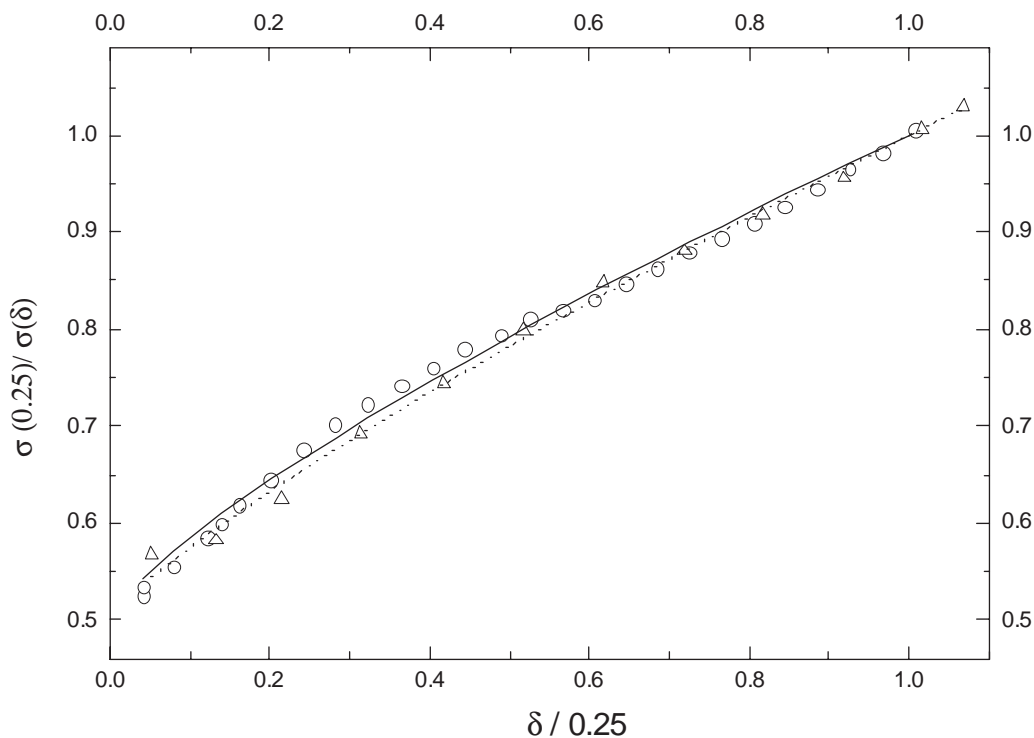


Fig. 3. Inverse of the ionic conductivity of copper selenide as a function of the deviation from stoichiometry. Both quantities are normalized to the values corresponding to non-stoichiometry  $\delta = 0.25$ . Circles and triangles represent the data from Ref. [6] for 452 and 520 K, respectively. Full and dashed lines represent best fits according to Eq. (4) for 452 K ( $\alpha = 0.775$ ) and 520 K ( $\alpha = 0.825$ ), respectively.

in Eq. (3),

$$\frac{dt(\mu_0 - \mu_G)\Omega_{Cu}\sigma_G}{dL e^2} = \frac{x_1}{2R} \int_0^1 d\left(\frac{x}{x_1}\right) \left(1 + D^z \left(\frac{x}{x_1}\right)^\alpha\right) + \frac{L}{2} \int_{x_1/L}^1 d\left(\frac{x}{L}\right) \times \left(1 + \left(D + (1 - D) \frac{(x/L) - (x_1/L)}{1 - (x_1/L)}\right)^\alpha\right), \quad (6)$$

where  $R = \bar{S}_1/S_2$  and  $D = \delta(x_1)/\delta_G$ .  $D$  vs.  $L$  dependence may be obtained by knowing that the ratio of chemical potentials drops along parts I and II is equal to the ratio of respective resistances, which is equal to the ratio of respective values of integrals in (6). Knowing also that in the case of parabolic valence band the width of which is composition independent, the chemical potential difference  $\mu_0 - \mu(\delta)$  is proportional to the  $\delta^{2/3}$  [6,7]. We obtain

$$\frac{\mu_0 - \mu(x_1)}{\mu(x_1) - \mu_G} = \frac{D^{2/3}}{1 - D^{2/3}} = \frac{\frac{x_1}{R} \cdot \left(1 + \frac{D^z}{\alpha + 1}\right)}{(L - x_1) \cdot \left(1 + \frac{1}{\alpha + 1} \cdot \frac{1 - D^{\alpha+1}}{1 - D}\right)}. \quad (7)$$

Condition (7) yields very accurate (square of correlation > 0.99999) approximate solution

$$D = \frac{1}{1 + a_1z + a_2z^2 + a_3z^3}, \quad (8)$$

where  $z = (L - x_1)R/x_1$  and  $a_1, a_2, a_3$  are coefficients taking values from the corresponding intervals (1.921, 1.942), (0.916, 0.928), (−0.096, −0.104), respectively, depending on the selected value of  $\alpha$  from its range of values,  $0.775 \leq \alpha \leq 0.825$ . With the same accuracy expression (6) may be rewritten in the form

$$\frac{dt}{dL} \gamma = \frac{x_1}{2R} \left( \frac{\alpha + 2}{\alpha + 1} z + 1 + \frac{b_1}{\alpha + 1} + \frac{b_2}{(1 + b_3z)^{b_4}} \right), \quad (9)$$

where

$$\gamma = \frac{1}{e} \text{EMF}(T_G, \delta_G) \frac{d^3(T_G, \delta_G)}{4 \cdot (2 - \delta_G)} \sigma_{iG}(T_G, \delta_G). \quad (10)$$

Here  $\text{EMF} = (\mu_0 - \mu_G)/e$ , and  $b_1, b_2, b_3, b_4$  are parameters taking values from the corresponding intervals (0.197, 0.199), (0.803, 0.801), (0.563, 0.617), (1.584, 1.572), respectively, for the selected values of  $\alpha$  from its range of values  $0.775 \leq \alpha \leq 0.825$ .

The monitoring of the process of growth starts at  $t = t_0, L = L_0 > x_1$ , when the sample already fills the entire cross-section of quartz tube and finishes at  $t, L = L_0 + l$ . Measured from Cu plate  $L_0 \approx 600$  pixels  $\cong 3.4$  mm (1 mm = 176 pixels). The maximum value of  $l$  was around 10 mm corresponding to the range of homogeneity of the temperature gradient within the furnace. The integration of Eq. (9) finally gives

$$(t - t_0)2\gamma = \frac{1}{2} \frac{\alpha + 2}{\alpha + 1} l^2 + \left[ \frac{\alpha + 2}{\alpha + 1} (L_0 - x_1) + \frac{x_1}{R} \left(1 + \frac{b_1}{\alpha + 1}\right) \right] l + \left(\frac{x_1}{R}\right)^2 \frac{b_2}{b_3(\alpha + 1)(b_4 - 1)} \left(1 + b_3 \frac{L_0 - x_1}{x_1} R\right)^{1-b_4} \times \left(1 - \left(1 + \frac{l}{(x_1/b_3R) + (L_0 - x_1)}\right)^{1-b_4}\right). \quad (11)$$

Using values 0.775 and 0.825 for  $\alpha$ , together with corresponding  $b_i$ , we fit our experimental results  $t$  vs.  $l$  using Eq. (11) allowing four free fitting parameters. In this way, we obtain for  $\alpha = 0.775$  (see Fig. 4)  $t_0 = 11353$  s,  $\gamma = 420$  pixels<sup>2</sup>/s = 0.0136 mm<sup>2</sup>/s,  $L_0 - x_1 = 550$  pixels,  $x_1/R = 7400$  pixels. We estimated the fitting parameter  $x_1/R$  by observing the sprouting stage of growth. We recorded a period of about 80 min of flat growing surface crossing almost full monitor screen of about 420 pixels ( $\approx 2.4$  mm). By the help of expression (6), by noting that for that period of growth the second integral is very small and by using the extrapolated value of  $\gamma = 0.0148$  mm<sup>2</sup>/s = 458 pixels<sup>2</sup>/s one obtains  $x_1/R = 6730$  pixels.

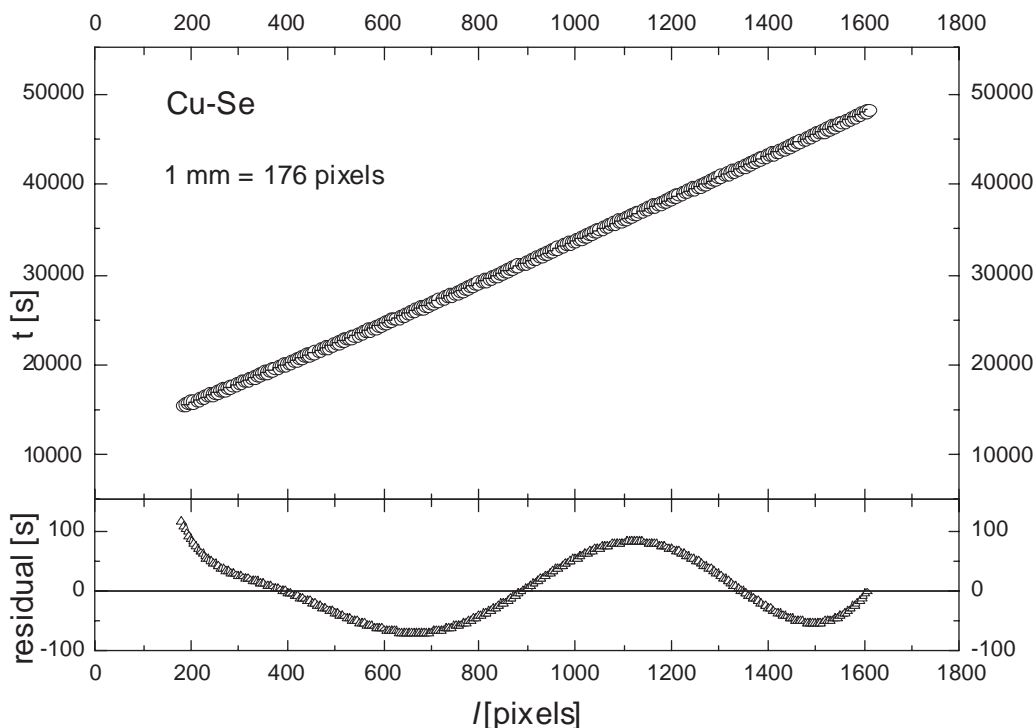


Fig. 4. Growth of copper selenide crystal. *Upper panel*: Time of crystal growth ( $t$ ) as a function of the length of growing crystal ( $l$ , as measured from  $L_0$ ). Circles: measured data; line: best fit according to Eq. (11) with  $\alpha = 0.775$ . *Lower panel*: Fit residuals (triangles) as a function of crystal length.

This is in very good agreement with the value obtained from fitting procedure.

Since the maximum value of  $l$  does not exceed 1600 pixels, and  $L_0 \approx 600$  pixels the last term in Eq. (11) may be expanded (using the expected value of  $x_1$  between 50 and 150 pixels as well) into a power series in  $l/M$  ( $M = 1 + b_3(L_0/x_1 - 1)$ ,  $R \approx 11900$  pixels). Since the quadratic term of the expansion contributes less than 2% to the series we retain the linear term only, and obtain

$$(t - t_0)2\gamma = \frac{1}{2} \left( \frac{\alpha + 2}{\alpha + 1} \right) l^2 + Pl, \quad (12)$$

$$P = \frac{\alpha + 2}{\alpha + 1} (L_0 - x_1) + \frac{x_1}{R} \left( 1 + \frac{b_1 + b_2}{\alpha + 1} \right),$$

expression (12) may equivalently be used to fit experimental growth results obtained in the experiments in which the inevitable sprouting part

of the grown crystal enables the power series expansion of Eq. (11). This expansion makes the final, quadratic, dependence of  $t$  on  $l$  much simpler, just as it turns out to be in the case of the growth of non-stoichiometric mixed conductor materials (cf. the Ag–Se system of the next section). There are three parameters to fit:  $t_0$ ,  $\gamma$  and  $P$ . The fitting procedure yields

$$\begin{aligned} \gamma &= 415.0(419.3) \text{ pixels}^2/\text{s} = 0.0134(0.0135) \text{ mm}^2/\text{s}, \\ P &= 17694(17876) \text{ pixels and } t_0 = 11568.5(11568.4)\text{s} \\ &\text{for } \alpha = 0.825(0.775). \end{aligned}$$

Before we comment the results of fitting and present the magnitude of the ionic conductivity, which can be easily deduced from the value of  $\gamma$ , we must emphasize once again that the evaluation of the  $t$  vs.  $l$  dependence (12) was made under certain approximations. To be more certain about

the use of this growth method as a method of determination of  $\sigma_i$  one should select a system in which the ionic conductivity distribution along the axis of a grown sample is well known. We decided to perform the growth of the silver selenide system,  $\text{Ag}_{2+\delta}\text{Se}$ . This material is as similar as possible to Cu–Se, and, what is crucial, its ionic conductivity is independent on composition and therefore on the axial coordinate as well.

#### 4. Ag–Se system

Ag–Se system has been thoroughly explored by Rom and Sitte [10] in the sense that electronic and ionic conductivity, as well as diffusivity, have been carefully measured as functions of composition or non-stoichiometry in the range from  $\text{Ag}_{2.0030}\text{Se}$  (sample in equilibrium with silver) to  $\text{Ag}_{1.9992}\text{Se}$  (in equilibrium with selenium) at 433 K. The temperature dependence of ionic conductivity using polarization method has been determined on strictly stoichiometric samples from 433 up to 623 K. Earlier results of Myatani [11] and Okazaki [12] are 30% higher than the results in Ref. [10] although the similar activation energies have been reported.

The structure of silver selenide superionic ( $\alpha$ ) phase is body-centered cubic (Im3m) in which Se atoms form a bcc cage, creating in this way open {110} channels for Ag atoms diffusion. Since these channels are built by face sharing tetrahedra, the activation energy for ionic conductivity or diffusivity is, as expected, about twice smaller than that in cuprous selenide (Fm3m) in which the diffusion paths are of {110} type including alternating face sharing tetrahedra and octahedra.

On the basis of the table in Ref. [9], by using the usual description of the ionic conductivity temperature dependence.

$$\sigma_i T = A e^{-(E/kT)} \quad (13)$$

the activation energy for  $\text{Ag}_2\text{Se}$  is calculated to be 9.395 kJ/mol ( $E/k = 1130$  K) and  $A = 1.203 \times 10^6$  S/m K.

Since it has been shown [10] that  $\sigma_i$  is within 10% composition independent, it is independent on any composition distribution along the axis of grown

sample, and thus independent on  $x$ , the evaluation of integral (3) is straightforward yielding

$$\frac{dt}{dL}\gamma = L + x_1 \left( \frac{S_2}{\bar{S}_1} - 1 \right) + l^* \frac{S_2}{S^*}, \quad (14)$$

where  $S^*$ ,  $\bar{S}_1$  and  $S_2$  are the cross-section of polycrystalline silver selenide, average cross-section of the transition region where sprouting crystal threads grow, and cross-section of fully realized growth in tube, respectively. By integrating from  $L_0$  to  $L_0 + l$  we obtain

$$t = t_0 + \frac{l^2}{2\gamma} + \frac{l}{\gamma} K,$$

$$K = L_0 + l^* \frac{S_2}{S^*} + x_1 \left( \frac{S_2}{\bar{S}_1} - 1 \right), \quad (15)$$

Very good fit of the experimental data during the almost 13 mm of growth can be obtained using Eq. (15). It is shown in Fig. 5 together with fit residuals. The values of the relevant parameters obtained are:  $\gamma = 665 \text{ pixels}^2/\text{s} = 0.0215 \text{ mm}^2/\text{s}$  and  $K = 5100$  pixels.

The growth experiment has been performed at 760 K. In order to compare the value of  $\sigma_i$  obtained from the presented fit with the one obtained from the extrapolation of the measurements [10], we have to extract the value of the ionic conductivity from the obtained value of  $\gamma$  using expression (10). To make this properly, one has to know the dependences of electromotive force, EMF, and lattice parameter,  $a$ , on temperature, and the fact that Ag–Se unit cell contains  $2 \times 2 = 4$  Ag atoms. The values of both may only be obtained by extrapolation. Linear extrapolation of  $a$  vs.  $T$  data of Ref. [13] yields the value 0.508 nm for  $a$  at 760 K. The value of EMF at 760 K may be obtained on the basis of the value 0.275 V at 433 K [10] corrected by  $\partial \text{EMF} / \partial T$  vs.  $T$  data of Ref. [14], which finally yields 0.300 V. Together with the ionic conductivity value of 0.358 S/mm at 760 K using formula (13) with 1 mm = 176 pixels one obtains  $\gamma = 0.0220 \text{ mm}^2/\text{s} = 682 \text{ pixels}^2/\text{s}$ . We observed the value  $\gamma = 665 \text{ pixels}^2/\text{s} = 0.0215 \text{ mm}^2/\text{s}$ , which is only 2.5% lower than the expected one.

The value of the third parameter  $K$  is within the expected limits since beside the measurable values of  $L_0 = 600$  pixels,  $l^* \approx 2$ ,  $r^* \approx 3$ , and

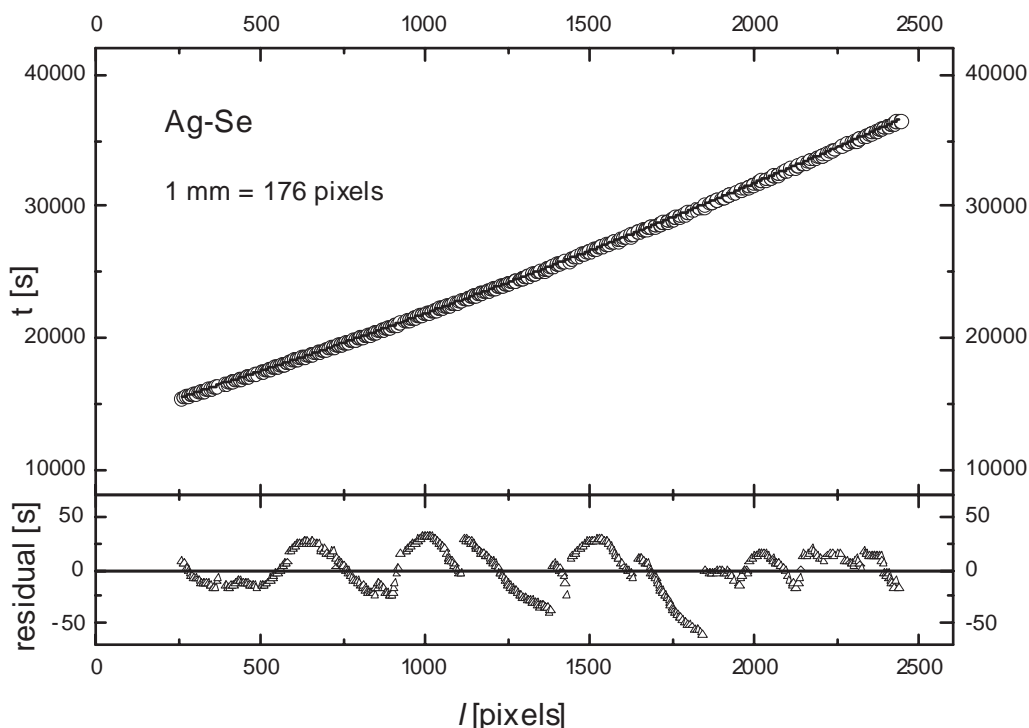


Fig. 5. Growth of silver selenide crystal. *Upper panel*: Time of crystal growth ( $t$ ) as a function of the length of growing crystal ( $l$ , as measured from  $L_0$ ). Circles: measured data; line: best fit according to Eq. (15). *Lower panel*: Fit residuals (triangles) as a function of crystal length.

$r_2 = 1$  mm, and our reasonable guess of  $x_1 \approx 100$  pixels we obtain the ratio of effective cross-section area of the sprouting part and homogeneous one being  $\frac{1}{46}$  that fits well the expectation value of  $\frac{1}{50}$  evaluated on the basis of the observed initial growth rate.

## 5. Cu–Se system

As we have already discussed [4] there is a problem of reliable data on the ionic conductivity (or diffusivity) of non-stoichiometric cuprous selenide in the temperature and composition range where the ECS crystals are usually grown, i.e., between 600 and 830 K, and at the non-stoichiometry of around  $\delta = 0.25$ . The ultimate choice is the extrapolation of  $\sigma_i$  vs.  $T$  on the basis of the results of our own experiments [6,7] (up to 520 K and up to  $\delta = 0.26$ ) that have been shown to agree well with those of Ref. [15] (up to 410 K). The

extrapolation is achieved by formula  $\sigma_i(T, 0.25) = 1.94 \times 10^6 / T \exp(-2018/T)$  S/m. It is shown to be valid in the superionic phase from 413 to 520 K [6]. At the growth temperature of 760 K and at  $\delta \approx 0.25$ , the estimated value of  $\sigma_i$  is 179.3 S/m.

The extrapolated ionic conductivity value at 760 K should be compared to the data from Ref. [16] measured between 580 and 970 K in the composition range between  $\delta = 0$  and 0.18. The results in Ref. [16] are presented in the composition range narrower than the range of existence of homogenous  $\alpha$  phase [17]. This is not surprising since the measurements were done in an open volume assembly and therefore with permanent loss of selenium by evaporation during the experiment. According to Ref. [18] the Se equilibrium pressure is strongly composition dependent, ranging from  $10^{-14}$  to  $10^{-10}$  atm for nearly stoichiometric samples, up to  $10^{-5}$ – $10^{-1}$  atm for maximum non-stoichiometric samples. The higher the deviation from stoichiometry, the

higher is the Se vapor pressure and the longer is the time needed to measure (achieve) real ionic conductivity value using the polarization measuring method. The reliability of the observed  $\sigma_i$  values decreases as non-stoichiometry increases, and it apparently becomes useless above certain limits [16].

We are now able to discuss the results obtained by fitting the experimental  $t$  vs.  $l$  curve using either Eq. (11) or Eq. (12). At temperature of our growth experiment of 760 K the lattice parameter value may be found to be 0.582 nm, by extrapolation of the data of Refs. [4,19]. EMF value of 0.468 V is obtained from existing data [4,20] extrapolated to 760 K. Together with the value of ionic conductivity, extrapolated according to Refs. [4,6], of 179.3 S/m, the value of  $\gamma$  of 0.0148 mm<sup>2</sup>/s = 458 pixels<sup>2</sup>/s is obtained by using expression (10). This value has to be compared to the value  $\gamma = 409\text{--}419$  pixels<sup>2</sup>/s = 0.0132–0.0135 mm<sup>2</sup>/s corresponding to the parameter  $\alpha$  lying between 0.825 and 0.775, obtained from the experiment using the described fitting procedure.

Considering the results of both silver and copper selenide experiments, we may say that there is a significant degree of agreement between calculated and measured values of the coefficient  $\gamma$ .  $\gamma$  is a complex coefficient since it contains extrapolated values of EMF and lattice parameter. Having in mind the approximations made in deriving the equation of growth for the copper selenide and the fitting procedure, the agreement is very good. We may draw two conclusions. First, the overestimation obtained in the growth rate determination [4] is definitely not related to the value of  $\sigma_i$  used. It is now clear that the cause of the overestimation lies in factor GF of Eq. (2), i.e., in the effect of pure geometry and/or nucleation resistance related to the average single crystal surface structure. Second, our growth method appears to be successful in obtaining a very good estimation of the ionic conductivity, provided one controls the geometry and the polycrystallinity of the growing interface. (The high temperature extrapolated data on ionic conductivity of cuprous selenide measured up to 523 K [7] might be regarded as correct within 10%.) This is very encouraging since there are

substantial difficulties in measurements of the ionic part of the electric conductivity in mixed ionic conductors above the temperatures for which the measured data exist (523 K for Cu- and 623 K for Ag-mixed conductors), up to the melting temperature, since on these temperatures the materials that provide the electron current blockade in those measurements (such as AgI and CuBr) disintegrate. The only method left includes total electric conductivity measurements from which the magnitude of the ionic part (of order of 0.1%) can be extracted. The error in thus estimated ionic conductivity value is at least 100%, while the error of the method proposed here is 10% at most.

## References

- [1] A.V. Babkin, H. Alles, P.J. Hakonen, A.Ya. Parshin, J.P. Ruutu, J.P. Saramäki, Phys. Rev. Lett. 75 (18) (1995) 3324;  
A.V. Babkin, H. Alles, P.J. Hakonen, J.P. Ruutu, J.P. Saramäki, A.Ya. Parshin, J. Low Temp. Phys. 101 (1995) 525.
- [2] M. Wortis, Equilibrium crystal shapes and interfacial phase transitions, in: R. Vanselow, R. Howe (Eds.), Chemistry and Physics of Solids Surfaces, Vol. 7, Springer, Berlin, 1988, pp. 367–405.
- [3] J. Gladić, Z. Vučić, D. Lovrić, J. Crystal Growth 242 (2002) 517.
- [4] Z. Vučić, J. Gladić, J. Crystal Growth 205 (1999) 136.
- [5] I. Yokota, J. Phys. Soc. Japan 16 (11) (1961) 2213.
- [6] M. Horvatić, I. Aviani, M. Ilić, Solid State Ionics 34 (1989) 21.
- [7] M. Horvatić, Z. Vučić, Solid State Ionics 13 (1984) 117.
- [8] T. Ohachi, B.R. Pamplin, J. Crystal Growth 42 (1977) 592.
- [9] T. Ohachi, I. Taniguchi, J. Crystal Growth 40 (1977) 109.
- [10] I. Rom, W. Sitte, Solid State Ionics 101–103 (1997) 381.
- [11] S. Miyatani, Solid State Commun. 38 (1981) 257.
- [12] H. Okazaki, J. Phys. Soc. Japan 23 (1967) 355.
- [13] M. Oliveria, R.K. McMullan, B.J. Wuensch, Solid State Ionics 28–30 (1988) 1332.
- [14] T. Ohachi, I. Taniguchi, J. Crystal Growth 3/4 (1981) 89.
- [15] T. Ishikawa, S. Miyatani, J. Phys. Soc. Japan 42 (1) (1977) 159.
- [16] P.N. Inglizjan, T.P. Jorga, N.S. Chhenkeli, Izv. Akad. Nauk SSSR, Neorg. Mater. 20 (1984) 1763.
- [17] R.D. Heyding, Can. J. Chem. 44 (1966) 1233.
- [18] H. Rau, A. Rabenau, J. Solid State Chem. 1 (1970) 515.
- [19] A. Tonejc, Z. Ogorelec, B. Mestnik, J. Appl. Crystallogr. 8 (1975) 375.
- [20] M. Horvatić, Z. Vučić, J. Gladić, M. Ilić, I. Aviani, Solid State Ionics 27 (1988) 31.